2010

Using NMR Metabolomics to Investigate Tricarboxylic Acid Cycle-dependent Signal Transduction in *Staphylococcus epidermidis*

Marat R. Sadykov
University of Nebraska—Lincoln

Bo Zhang
University of Nebraska-Lincoln

Steven M. Halouska
University of Nebraska-Lincoln, halouska@huskers.unl.edu

Jennifer L. Nelson
University of Nebraska, Lincoln

Lauren W. Kreimer
University of Nebraska, Lincoln

See next page for additional authors

THE JOURNAL OF BIOLOGICAL CHEMISTRY VOL. 285, NO. 47, pp. 36616–36624, November 19, 2010

Using NMR Metabolomics to Investigate Tricarboxylic Acid Cycle-dependent Signal Transduction in *Staphylococcus epidermidis*[*] [S]

Received for publication, June 8, 2010, and in revised form, September 21, 2010 Published, JBC Papers in Press, September 22, 2010, DOI 10.1074/jbc.M110.152843

Marat R. Sadykov[‡], Bo Zhang[§], Steven Halouska[§], Jennifer L. Nelson[‡1], Lauren W. Kreimer[¶], Yefei Zhu[‡], Robert Powers[§2], and Greg A. Somerville[‡3]

From the [‡]School of Veterinary Medicine and Biomedical Sciences, University of Nebraska, Lincoln, Nebraska 68583-0905, the [§]Department of Chemistry, University of Nebraska, Lincoln, Nebraska 68588-0304, and the [¶]Department of Biochemistry, University of Nebraska, Lincoln, Nebraska 68588-0664

Staphylococcus epidermidis **is a skin-resident bacterium and a major cause of biomaterial-associated infections. The transition from residing on the skin to residing on an implanted biomaterial is accompanied by regulatory changes that facilitate bacterial survival in the new environment. These regulatory changes are dependent upon the ability of bacteria to "sense" environmental changes. In *S. epidermidis*, disparate environmental signals can affect synthesis of the biofilm matrix polysaccharide intercellular adhesin (PIA). Previously, we demonstrated that PIA biosynthesis is regulated by tricarboxylic acid (TCA) cycle activity. The observations that very different environmental signals result in a common phenotype (*i.e.* increased PIA synthesis) and that TCA cycle activity regulates PIA biosynthesis led us to hypothesize that *S. epidermidis* is "sensing" disparate environmental signals through the modulation of TCA cycle activity. In this study, we used NMR metabolomics to demonstrate that divergent environmental signals are transduced into common metabolomic changes that are "sensed" by metabolite-responsive regulators, such as CcpA, to affect PIA biosynthesis. These data clarify one mechanism by which very different environmental signals cause common phenotypic changes. In addition, due to the frequency of the TCA cycle in diverse genera of bacteria and the intrinsic properties of TCA cycle enzymes, it is likely the TCA cycle acts as a signal transduction pathway in many bacteria.**

Staphylococcus epidermidis is a skin-resident, opportunistic pathogen that is the leading cause of hospital-associated infections (1). Although the type and severity of diseases produced by this bacterium varies, its most common infectious manifestation is associated with implanted biomaterials. The dramatic environmental changes that occur during the transition from being skin-resident to residing on implanted biomaterials necessitates the need for changes in the expression of genes coding for enzymes required for growth in the new environment. This environmental adaptation often includes activating transcription of virulence genes; hence, most virulence genes are regulated by environmental and nutritional signals (2). Accordingly, a major area of interest in microbiology is determining how bacteria "sense" and respond to environmental signals. Given the tremendous diversity of microbial life, it is not surprising that the mechanisms bacteria employ are equally diverse. These mechanisms include two-component regulatory systems, alternative σ factors, mechanosensors, small RNAs, riboswitches, and many others. Although remarkable advances have been made in identifying the response regulators, our knowledge of signaling mechanisms has lagged behind, the exception being cell-density signaling.

The tricarboxylic acid (TCA) cycle has been implicated as regulating or affecting staphylococcal virulence and/or virulence determinant biosynthesis (3–9). The TCA cycle has three primary functions: (i) to provide biosynthetic intermediates, (ii) to generate reducing potential, and (iii) to directly produce a small amount of ATP. The availability of biosynthetic intermediates affects the availability of amino acids and nucleic acids. Increasing the reducing potential alters the bacterial redox balance, necessitating oxidation reactions via the electron transfer chain. The small amount of ATP produced directly by the TCA cycle is amplified many times when the ATP generated by oxidative phosphorylation is considered. In short, the TCA cycle has a central function in maintaining the bacterial metabolic status. Importantly, the activity of TCA cycle enzymes is affected by the availability of nutrients and a variety of stress-inducing stimuli (9–12); thus, the availability of biosynthetic intermediates, the redox status, and the energy status can be altered by nutritional and environmental stimuli. These observations led us to propose a fourth function for the TCA cycle, the transduction of external signals into intracellular metabolic signals that can be "sensed" by metabolite-responsive regulatory proteins (2). Fundamental to this hypothesis are the predictions that disparate environmental stimuli will cause common metabolic changes and that these metabolic changes will precede regulatory changes.

Two of the more extensively studied environmental stimuli that influence *S. epidermidis* virulence determinant biosynthe-

* This manuscript is a contribution of the University of Nebraska Agricultural Research Division, supported in part by funds provided through the Hatch Act and from National Institutes of Health Grant AI087668 (to G. A. S.) and the American Heart Association Grant 0860033Z (to R. P.).
[S] The on-line version of this article (available at http://www.jbc.org) contains supplemental Fig. S1.
[1] Present address: Dept. of Microbiology, Cornell University, Ithaca, NY 14853.
[2] To whom correspondence may be addressed: 722 Hamilton Hall, Lincoln, NE 68588-0304. Fax: 402-472-9402; E-mail: rpowers3@unl.edu.
[3] To whom correspondence may be addressed: 155 VBS, Fair St. and East Campus Loop, Lincoln, NE 68583-0905. Fax: 402-472-9690; E-mail: gsomerville3@unl.edu.

sis are iron limitation (13, 14) and ethanol stress (15, 16). The effect of iron limitation on bacterial growth is primarily through preventing the activity of enzymes that require iron as a cofactor and altering transcription of iron-regulated genes (2). As *S. epidermidis* has many iron-requiring enzymes (*e.g.* aconitase, serine dehydratase, peptide deformylase, iron-containing alcohol dehydrogenase, nitrate reductase, etc.), it is reasonable to expect that the metabolic effects of iron-limited growth are diverse and not restricted to the TCA cycle. Ethanol denatures proteins in the cytoplasmic membrane, causing changes in membrane permeability, which can lead to the loss of membrane integrity (17). With the exception of the succinate dehydrogenase complex, most TCA cycle enzymes are not membrane-associated; hence, it is reasonable to predict that the deleterious effects of ethanol stress are largely independent of the TCA cycle. Taken together, these observations suggest that disparate environmental conditions will cause divergent metabolomic changes. In contrast to this suggestion, our central hypothesis predicts that different stresses will cause common metabolomic changes that are dependent on the TCA cycle. To test our central hypothesis, we chose to induce environmental stress by growing bacteria in an iron-limited medium or in a medium containing ethanol and assessing the metabolic changes using NMR metabolomics.

EXPERIMENTAL PROCEDURES

Bacterial Strains, Media, and Growth Conditions—*S. epidermidis* wild-type strain 1457 (18) and the isogenic aconitase mutant strain 1457-*acnA*::*tetM* (*tetM* cassette inserted into position 856 of the 2,702-bp *acnA* gene) and σ^B mutant strain 1457-*sigB*::*dhfr* (7, 19) have been described. Strains 1457-*codY*, 1457-*ccpA*, 1457-*acnA-codY*, and 1457-*acnA-ccpA* were constructed using the gene splicing by overlap extension (gene SOEing) technique (20) to replace the gene of interest with an antibiotic resistance marker (*i.e. ermB* or *tetM*). Primers were designed to amplify ~1-kb regions upstream and downstream of the gene of interest based on the genome sequence of *S. epidermidis* strain RP62A. Gene knockouts were confirmed by PCR and Southern blot hybridization. In addition, strains containing mutations in the single *S. epidermidis* aconitase gene were assayed to ensure that no aconitase activity was detected (data not shown). All strains were grown in tryptic soy broth without dextrose (TSB;[4] BD Biosciences) supplemented with 0.25% glucose (Sigma) or 0.25% $^{13}C_6$-glucose (Cambridge Isotope Laboratories). Deferrated TSB (DTSB) was prepared by adding 50 g of Chelex 100 (Sigma) to ~1 liter of TSB and stirring at 4 °C for 20 h. After 20 h, the Chelex resin was removed, 1 mM $MgSO_4$ was added, the volume was adjusted to 1 liter, and the medium was filter-sterilized. To induce ethanol stress and minimize growth defects, ethanol or deuterated ethanol (Isotec) was added to the medium at a final concentration of 4% (v/v). All cultures were inoculated 1:200 from overnight cultures (normalized for growth) into glucose supplemented TSB, incubated at 37 °C, and aerated at 225 rpm with a flask-to-medium ratio of 7:1. Bacterial growth was assessed by measuring the optical density at 600 nm (A_{600}). Antibiotics, when used, were purchased from Fisher Scientific or Sigma and used at the following concentrations: chloramphenicol (8 μg/ml), trimethoprim (10 μg/ml), and erythromycin (8 μg/ml).

Aconitase Activity Assay—Cell-free lysates of *S. epidermidis* were prepared as follows. Aliquots (3 ml) were harvested by centrifugation (1 min at 20,800 × *g*) at the indicated times, suspended in 1.5 ml of lysis buffer containing 90 mM Tris (pH 8.0) and 100 μM fluorocitrate. The samples were lysed in 2-ml screw cap tubes containing lysing matrix B using a FastPrep instrument (MP Biomedicals). The lysate was centrifuged for 5 min at 20,800 × *g* at 4 °C. Aconitase activity in the resulting cell-free lysate was assayed by the method described by Kennedy *et al.* (21). One unit of aconitase activity is defined as the amount of enzyme necessary to give a ΔA_{240} min^{-1} of 0.0033 (22). Protein concentrations were determined by the Lowry method (23).

Northern Blot Analysis—Northern blot analysis of transcripts was performed as described (7). Oligonucleotide primers used in making DNA probes were designed using the *S. epidermidis* RP62A genome sequence. Probes for Northern blotting were generated by PCR amplification of unique internal regions of RNAIII and *glnA* (*femC*) genes using the following primers: femC, forward, 5′-GATGTTTGATGGTTCATCTATTGAAGGTTTCG-3′; femC, reverse, 5′-GCAGTATCAGTCAATTGTAAATCACCTTCAG-3′; RNAIII, forward, 5′-TGAAAAATTTGCTTAATCTAGTCGAGTG-3′; and RNAIII, reverse, 5′-CATGATAAATTGAATGTTGTTTACGATAGC-3′.

DNA probes were labeled using the North2South random prime labeling kit (Pierce). Electrophoresis, transfer of the RNA to the Nytran SPC nylon membrane (Whatman), and hybridization were done using the NorthernMax kit (Ambion). Detection was performed using the chemiluminescent nucleic acid detection module (Pierce).

PIA Immunoblot Assay—PIA accumulation was determined as described (24).

NMR Sample Preparation—NMR samples for one-dimensional ^1H spectra were prepared from 10 independent, 25-ml *S. epidermidis* cultures. Two-dimensional ^1H-^{13}C HSQC (25, 26) and two-dimensional ^1H-^1H TOCSY (27) spectra were prepared from three independent 50-ml cultures. The TSB medium used in the two-dimensional ^1H-^{13}C HSQC analysis contained 0.25% $^{13}C_6$-glucose (Cambridge Isotope Laboratories). For two-dimensional ^1H-^{13}C HSQC and two-dimensional ^1H-^1H TOCSY involving ethanol stress, deuterated ethanol (Isotec) was used to minimize the contribution of exogenous ethanol to the NMR spectra. For one-dimensional ^1H NMR experiments, 2.74 A_{600} units were harvested at each time point, and for the two-dimensional ^1H-^{13}C HSQC and two-dimensional ^1H-^1H TOCSY experiments, 5.48 A_{600} units were collected. Bacteria were harvested by centrifugation (4,000 rpm for 5 min), suspended in 50 mM phosphate buffer in 100% D_2O at pH 7.2 (uncorrected), and lysed using lysing matrix B tubes and a FastPrep instrument. The lysates were centrifuged to remove cell debris and glass beads and then frozen in liquid nitrogen.

[4] The abbreviations used are: TSB, tryptic soy broth; DTSB, deferrated TSB; PIA, polysaccharide intercellular adhesin; HSQC, heteronuclear single quantum coherence; TOCSY, total correlation spectroscopy; PCA, principal component analysis; HPr, histidine-containing protein; CcpA, catabolite control protein A; PC, principal component.

All samples were kept at −80 °C until ready for analysis. At the time of use, a 600-μl aliquot of the cell-free lysate was transferred to each NMR tube.

NMR Analysis—The NMR spectra were collected on a Bruker 500-MHz Avance spectrometer equipped with a triple-resonance, *z* axis gradient cryoprobe. A BACS-120 sample changer with Bruker Icon software was used to automate the NMR data collection. The one-dimensional ^{1}H NMR spectra collection and principal component analysis (PCA) were performed as described with minor modifications (28–30). Briefly, each multidimensional NMR spectrum (chemical shifts and peak intensities) was converted to a single point in a multidimensional Cartesian space. Conceptually, each axis corresponds to a specific chemical shift, where the peak intensity is the value along the axis. PCA identifies a principal component vector ($\vec{P}_1$) corresponding to the largest variation in the data set within this multidimensional space. The second vector ($\vec{P}_2$) is orthogonal to the first and represents the next largest variation in the data set. Each successive vector describes a diminishing amount of the variability of the data set, where most of the variability is described by the first two principal components. The PC1 and PC2 scores (unitless values) are effectively the individual fit of each NMR spectrum to $\vec{P}_1$ and $\vec{P}_2$. The PC1 and PC2 scores are usually presented in a two-dimensional plot, where similar NMR spectra cluster together.

Solvent presaturation used excitation sculpting to efficiently remove the solvent and maintain a flat baseline, eliminating any need for baseline collection that may induce artifacts in the two-dimensional scores plot (31). Each NMR spectrum was center-averaged for PCA to minimize any experimental variations between cultures (32).

Two-dimensional ^{1}H-^{13}C HSQC spectra were collected and processed as described previously (7). Two-dimensional ^{1}H-^{1}H TOCSY spectra were collected with WATERGATE solvent presaturation (33) and a relaxation delay of 2 s. A total of 1,024 data points with a sweep width of 5,000 Hz and 256 data points with a sweep width of 5,001.324 Hz were collected in the direct and indirect ^{1}H dimensions, respectively. A total of 16 dummy scans and 8 acquisition scans were used to obtain each of the two-dimensional ^{1}H-^{1}H TOCSY NMR spectra. The two-dimensional ^{1}H-^{1}H TOCSY NMR spectra were processed similar to the two-dimensional ^{1}H-^{13}C HSQC spectra, and both spectra were analyzed using NMRView (One Moon Scientific (34)) and Sparky (71) to identify chemical shifts and assign peak intensities.

The observed NMR peaks in the two-dimensional ^{1}H-^{13}C HSQC and ^{1}H-^{1}H TOCSY spectra were assigned to specific metabolites using ^{1}H and ^{13}C chemical shift tolerances of 0.05 and 0.50 ppm, respectively, and the Madison Metabolomics Consortium Database (MMCD) (35), the BioMagResBank (36), and the Human Metabolome Database (37). The presence of metabolites and metabolic pathways were verified with the Kyoto Encyclopedia of Genes and Genomes (KEGG) (38) and the MetaCyc (39) databases.

Peak intensities were normalized for each two-dimensional NMR spectrum by dividing by the average peak intensity. The triplicate data sets were then used to calculate average intensities for each peak observed in the two-dimensional spectra for strain 1457, 1457-*acnA*, ethanol stress, and iron limitation. A percentage of error was calculated for each peak by dividing the standard deviation by the average peak intensity. The average peak intensities were then used to calculate a percentage of difference relative to the wild-type bacteria in TSB medium. Peaks with calculated percentage of differences greater than five times the average percentage of error were considered to have either decreased or increased concentrations relative to the wild-type strain 1457. Peaks with less than a 5-fold deviation were considered similar. Secondary peaks assigned to the same metabolite were required to have the same relative change in intensity to be classified as a metabolite with an increase or decrease in concentration.

Metabolomic Dendrogram—The relative clustering patterns in the PCA two-dimensional scores plots were quantitatively analyzed using a tree diagram and bootstrapping technique (40). The PC1 and PC2 scores for each set of 10 duplicate NMR spectra representing a specific metabolic state (iron limitation, ethanol treatment, etc.) were used to calculate an average PC score and standard deviation. Any PC scores outside 2 standard deviations were removed, and a new average was calculated. The average PC scores represent the center of a cluster of NMR spectra (metabolic state) in the two-dimensional scores plot. The process is repeated for each set of 10 duplicate NMR spectra. Distances between the average PC positions for each metabolic state are then calculated using the standard equation for a Euclidean distance to create a distance matrix.

To assess the significance of the similarity (overlap) or difference (separation) observed between pairs of clusters in the two-dimensional scores plot, standard bootstrapping methods were also applied (41, 42). Briefly, the average PC scores were recalculated by randomly selecting points from the data set. Distances were recalculated between the clusters using the new average PC scores to create a new distance matrix. The process was repeated until 100 different distance matrices were created and transferred to version 3.68 of the PHYLIP (43) suite of software programs. PHYLIP calculates a tree for each distance matrix and then determines a consensus tree. The program calculates a bootstrap value for each node, which is simply the number of times the node appears in all 100 trees. Bootstrap values below 50% imply a statistically insignificant separation. Conversely, as the bootstrap number increases above 50%, the confidence in the tree branch or separation increases.

RESULTS

Disparate Environmental Stresses Create a Metabolic Block in the TCA Cycle—To determine whether ethanol stress and iron limitation alter TCA cycle activity, the specific activity of aconitase in *S. epidermidis* strain 1457 at 2 (exponential growth) and 6 h (post-exponential growth) after inoculation was assessed (Fig. 1). As expected, iron-limited growth and ethanol stress prevented the post-exponential growth phase increase in the specific activity of the iron-requiring enzyme aconitase, creating a metabolic block in the TCA cycle (Fig. 1). Although ethanol-stressed bacteria are in the post-exponential growth phase at 6 h after inoculation, their growth is slower, which slows the consumption of glucose, and excess glucose can repress transcription of TCA cycle genes. Irrespective of

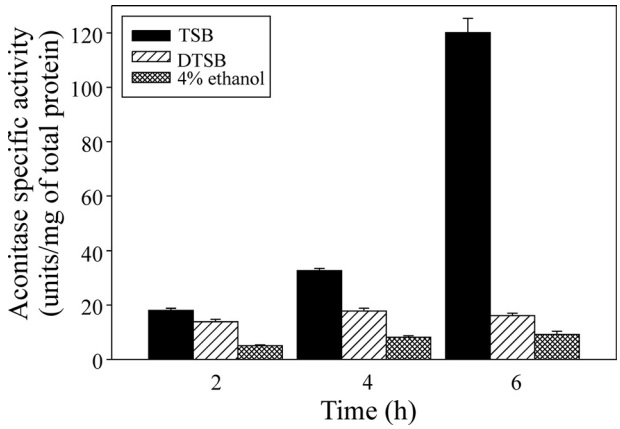

FIGURE 1. **The temporal induction of aconitase-specific activity is inhibited by dissimilar stressors.** Aconitase activity was assessed during the exponential (2 and 4 h) and post-exponential (6 h) growth phases during growth in DTSB or TSB containing 4% ethanol. The data are presented as the mean and S.E. of two independent experiments each determined in triplicate.

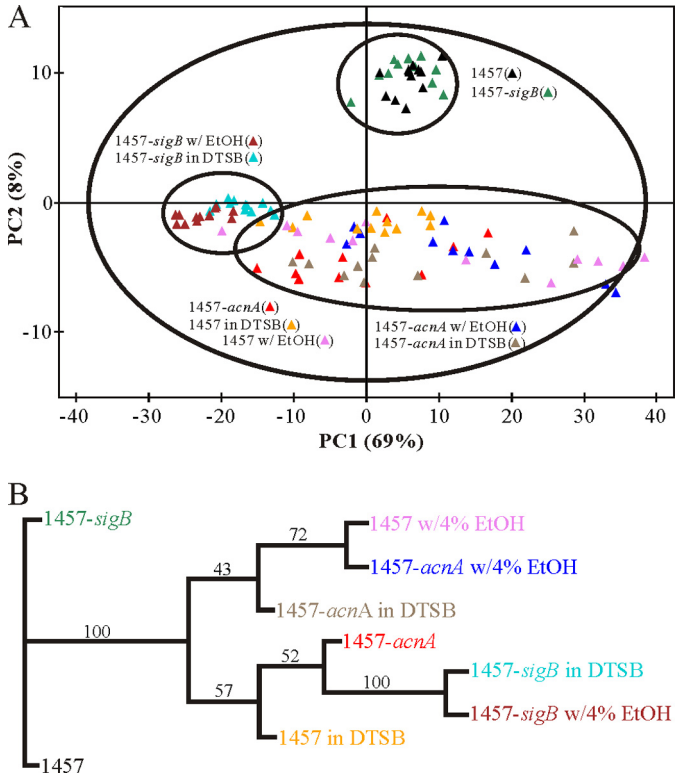

FIGURE 2. **Environmental stressors cause metabolomic perturbations similar to TCA cycle inactivation.** *A*, PCA two-dimensional scores plot comparing non-stressed, ethanol-stressed, or iron-limited cultures of strains 1457, 1457-*acnA*, and 1457-*sigB*::*dhfr* grown for 6 h. Symbols and colors are defined in the figure. The *ovals* are manually drawn to identify clusters of related samples and to guide the reader. They are not statistically relevant. The relative contribution of each principal component is indicated in the *parentheses*. *B*, metabolic tree generated using the PCA scores plot data demonstrating the relationship between stresses and strains. Bootstrap values are indicated on the dendrogram branches. Bootstrap values below 50% imply a statistically insignificant separation; conversely, as the bootstrap number increases above 50%, the confidence in the tree branch or separation increases.

the mechanism by which ethanol repressed aconitase-specific activity, the normal post-exponential growth phase increase in TCA cycle activity did not occur. These data demonstrate that environmental stresses whose deleterious effects are substantially different from one another have a similar effect on TCA cycle function.

Environmental Stimuli Elicit TCA Cycle-dependent Metabolic Changes—The TCA cycle provides biosynthetic intermediates, ATP, and reducing potential; therefore, alteration of TCA cycle activity will alter the metabolic status of a bacterium. To determine the metabolic changes associated with iron limitation, ethanol stress, and TCA cycle inactivation, NMR metabolomic analysis (28, 29) was used to assess the stressed and non-stressed metabolomes of strains 1457 and the TCA cycle inactive strain 1457-*acnA*. Specifically, *S. epidermidis* strains 1457 and 1457-*acnA* were grown for 2 or 6 h in TSB, TSB with 4% ethanol, or DTSB. Following acquisition of the NMR spectra, the table of integrals was used for PCA (Fig. 2*A*). As expected, during the exponential growth phase, PCA revealed that the effects of ethanol stress and iron limitation on the metabolome were largely independent of the TCA cycle (supplemental Fig. S1). This was expected due to the normal repression of TCA cycle activity during nutrient-rich growth (Fig. 1) (8, 44). Despite the TCA cycle being repressed during the exponential growth phase, the different stresses induced common metabolomic changes (Table 1). In contrast to the exponential growth phase, PCA of post-exponential growth phase metabolomes revealed that ethanol stress and iron limitation induced metabolomic changes very similar to TCA cycle inactivation (Fig. 2*A* and Table 2). In addition, these data highlight the relative insensitivity of the metabolome of strain 1457-*acnA* to ethanol stress and iron-limited growth, confirming that the major effect of these stressors is dependent upon the TCA cycle. That being said, the more diffuse clustering of ethanol-stressed metabolomes of both the wild-type and the aconitase mutant strains suggest that ethanol stress had TCA cycle-independent metabolomic effects (Fig. 2*A*). The TCA cycle-independent effects are likely due to the denaturation of membrane proteins not related to electron transport or the TCA cycle.

TABLE 1

Metabolites that have increased or decreased concentrations relative to the wild-type strain 1457 at 2 h after inoculation

Metabolites whose concentrations were changed under all stress conditions relative to the wild-type strain grown in TSB are shaded in gray.

Strain 1457[a] (DTSB) **Iron-limitation**	Strain 1457[a] (4% Ethanol) **Ethanol stress**	Strain 1457-*acnA*[a] (TSB) **TCA cycle inactivation**
Metabolites whose concentration is **increased** relative to strain 1457 grown in TSB medium.		
		Acetaldehyde
Acetyl-phosphate	Acetyl-phosphate	Acetyl-phosphate
		Citrate
		Glyceraldehyde
Metabolites whose concentration is **decreased** relative to strain 1457 grown in TSB medium.		
		Acetyl-glutamate[b]
		Asparagine
		Glutamate
	Lactate	Lactate
Glutamine	Glutamine	Glutamine
Succinate	Succinate	Succinate

[a] The intracellular concentration was considered to be increased or decreased when the percentage of difference in the NMR peak intensities was 5-fold greater than the percentage of error observed in the peak intensities between triplicate NMR spectra.

[b] Due to peak overlap, we are unable to determine whether the metabolite is acetyl-glutamine or acetyl-glutamate; however, we note that acetyl-glutamine is uncommon in prokaryotes.

Taken together, these data demonstrate that diverse environmental stimuli elicit common metabolic changes that require the TCA cycle.

TABLE 2

Metabolites that have increased or decreased concentrations relative to the wild-type strain 1457 at 6 h after inoculation

Metabolites whose concentrations were changed under all stress conditions relative to the wild-type strain grown inTSB are shaded in gray.

Strain 1457[a] (DTSB) **Iron-limitation**	Strain 1457[a] (4% Ethanol) **Ethanol stress**	Strain 1457-*acnA*[a] (TSB) **TCA cycle inactivation**
Metabolites whose concentration is **increased** relative to strain 1457 grown in TSB medium.		
Acetaldehyde	Acetaldehyde	Acetaldehyde
Acetate	Acetate	Acetate
Acetylalanine		
N-Acetyl-glucosamine	*N*-Acetyl-glucosamine	
	Acetyl-glucosamine 6-phosphate	
N-Acetyl-mannosamine	*N*-Acetyl-mannosamine	*N*-Acetyl-mannosamine
N-Acetyl-neuraminate	*N*-Acetyl-neuraminate	*N*-Acetyl-neuraminate
Acetyl-phosphate	Acetyl-phosphate	Acetyl-phosphate
		Arginine
		Citrate
Ethanol		
Glucosamine	Glucosamine[c]	Glucosamine
		Galactose-1-phosphate
GDP	GDP	
Glucose	Glucose	Glucose
Glucose-1-phosphate		
Glucose-6-phosphate	Glucose-6-phosphate	Glucose-6-phosphate
Glyceraldehyde	Glyceraldehyde	Glyceraldehyde
Lactate	Lactate	Lactate
	myo-Inositol	
		Proline
Ribose[c]	Ribose	Ribose
	UDP-*N*-acetyl-glucosamine	
Metabolites whose concentration is **decreased** relative to strain 1457 grown in TSB medium.		
α-Ketoglutarate	α-Ketoglutarate	α-Ketoglutarate
γ -Aminobutyrate	γ-Aminobutyrate	γ -Aminobutyrate
Acetyl-glutamate[b]	Acetyl-glutamate[b]	Acetyl-glutamate[b]
		Acetyl-ornithine
		Alanine
Arginine		
Asparagine	Asparagine	Asparagine
		Aspartate
β-Alanine	β-Alanine	β-Alanine
Citrulline	Citrulline	Citrulline
	Ethanol	Ethanol
Fructose-6-Phosphate	Fructose-6-Phosphate	Fructose-6-phosphate
Glutamate	Glutamate	Glutamate
Glutamine	Glutamine	Glutamine
Isocitrate	Isocitrate	Isocitrate
Methionine	Methionine	Methionine
NAD^+	NAD^+	
Ornithine	Ornithine	Ornithine
O-Succinyl-L-homoserine	O-Succinyl-L-homoserine	O-Succinyl-L-homoserine
Proline	Proline	
S-Adenosyl-L-methionine	S-Adenosyl-L-methionine	S-Adenosyl-L-methionine
Sedheptulose		
Selenomethionine	Selenomethionine	Selenomethionine
UDP-*N*-acetyl-glucosamine		

[a] The intracellular concentration was considered to be increased or decreased when the percentage of difference in the NMR peak intensities was 5-fold greater than the percentage of error observed in the peak intensities between triplicate NMR spectra.

[b] Due to peak overlap, we are unable to determine whether the metabolite is acetyl-glutamine or acetyl-glutamate; however, we note that acetyl-glutamine is uncommon in prokaryotes.

[c] The percentage of difference in the NMR peak intensities of these metabolites fell just below the 5-fold cutoff in the percentage of error observed in the peak intensities between the triplicate NMR spectra.

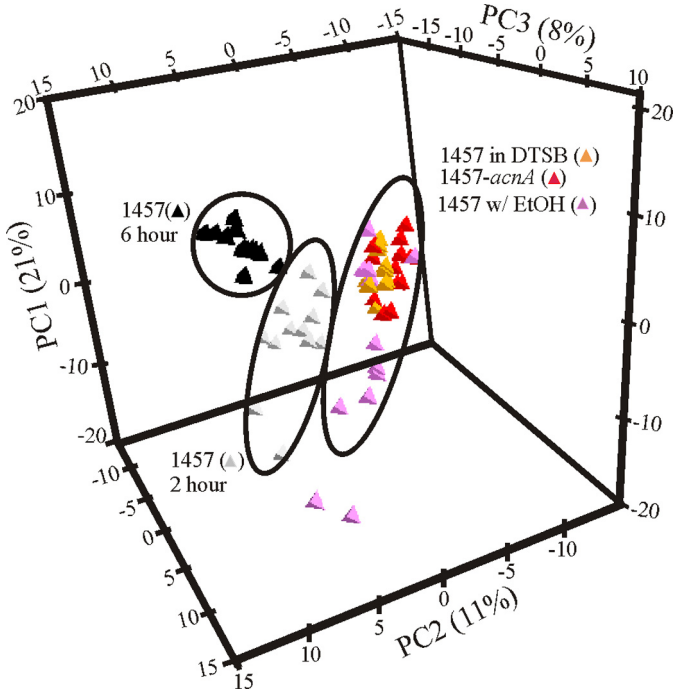

FIGURE 3. **PCA three-dimensional scores plot comparing non-stressed, ethanol-stressed, or iron-limited cultures of strains 1457 grown for 6 h with that of strain 1457 grown for 2 h.** Symbols and colors are defined in the figure. The *ovals* are manually drawn to identify clusters of related samples and to guide the reader. They are not statistically relevant. The relative contribution of each principal component is indicated within the *parentheses*.

The common metabolomic response to environmental stimuli can be more easily observed by a recently developed method to visualize PCA data (40). By calculating an average position for each data set, such that each PC value (PC1, PC2, etc.) is treated as an axis in a Cartesian coordinate system, a distance matrix can be generated. Correspondingly, methods developed for representing genetic distances in phylogenetic trees can be used to create a metabolomic dendrogram (43) (Fig. 2*B*). Using this approach, it becomes clear that stress-induced metabolomic responses are very similar to the metabolome of the aconitase-deficient strain 1457-*acnA*. As with the two-dimensional scores plot (Fig. 2*A*), the higher bootstrap values in the dendrogram for ethanol-stressed cultures also indicate that ethanol has TCA cycle-independent effects on the metabolome.

S. epidermidis grown in TSB under aerobic conditions have two distinct metabolic states: the nutrient-rich exponential phase and the nutrient-limited post-exponential phase. The transition from nutrient-rich conditions to nutrient-limited growth coincides with the transition from generating ATP by substrate-level phosphorylation to using oxidative phosphorylation. The reduced dinucleotides that drive oxidative phosphorylation are primarily derived from the TCA cycle; thus, inhibiting TCA cycle activity (Fig. 1) hinders the transition to oxidative phosphorylation and the post-exponential growth phase (8, 44). Iron-limited growth of strain 1457 or aconitase inactivation did not significantly alter the growth rate, although aconitase inactivation did increase the lag phase (data not shown). Both aconitase inactivation and iron-limited growth caused an early entry into the stationary phase; as such, the growth yield was decreased. As stated, the addition of 4% ethanol decreased the growth rate; therefore, it slowed the consumption of glucose. Based on these observations, it was reasonable to hypothesize that post-exponential growth phase (6 h)-stressed metabolomes will be more similar to an unstressed exponential growth phase (2 h) metabolome than to the unstressed metabolome of post-exponential growth phase of cultures. As expected, PCAs of unstressed strain 1457 cultures, grown for 2 or 6 h, form separate subsets in a three-dimensional scores plot (Fig. 3). Consistent with our hypothesis, PCAs of post-exponential growth phase-stressed and *acnA* mutant cultures were more closely associated with the unstressed exponential growth phase metabolome of strain 1457 than with the

strain 1457 post-exponential growth phase metabolome (Fig. 3). These data suggest that any stress that interferes with TCA cycle function results in a metabolome similar to an unstressed exponential phase culture.

Metabolomic Changes Are Largely Independent of the σ^B-mediated General Stress Response—In staphylococci, σ^B controls the general stress response and as such is activated during stress conditions, growth phase transitions, and morphological changes (45, 46). As stated previously, the regulation of many virulence determinants is affected by environmental stresses; therefore, the stress-dependent activation of σ^B has been an important area of research into the environmental regulation of staphylococcal virulence determinants (47–49). Interestingly, σ^B does not directly respond to most environmental signals, suggesting another path to transduce stress signals that is independent of σ^B. To test this possibility, an *S. epidermidis sigB* mutant strain (1457-*sigB*::*dhfr*) (19) was grown for 2 or 6 h in TSB, TSB with 4% ethanol, or DTSB and the metabolomes were analyzed by NMR spectroscopy. The PCA scores plot demonstrates that the majority of metabolomic changes associated with iron limitation and ethanol stress occur largely independent of σ^B (Fig. 2*A*). Additionally, the metabolomic dendrogram confirms that the stressor-induced metabolic changes observed in strain 1457-*sigB*::*dhfr* are most closely associated with those in the TCA cycle mutant strain 1457-*acnA* (Fig. 2*B*). Taken together, these data demonstrate that environmental stresses can alter the staphylococcal metabolome by a largely σ^B-independent mechanism that requires the TCA cycle.

Metabolomic Changes Precede Genetic Changes—Metabolomic data demonstrate that ethanol stress, iron limitation, and TCA cycle inactivation decrease the intracellular concentration of Gln relative to the wild-type strain grown in TSB medium (Tables 1 and 2). The two more likely explanations for the decreased intracellular concentration of Gln are: (i) the stressors alter enzymatic activity, causing a decrease in the concentration of Gln; or (ii) the stressors decrease transcription of genes involved in the biosynthesis of Gln, resulting in a decreased concentration of Gln. If the first possibility is correct, then stressors will cause an increase in the transcription of Gln biosynthetic genes as bacteria attempt to compensate for the decreased availability of Gln. If the second possibility is correct, then stressors will cause a decrease in the transcription of Gln biosynthetic genes. To determine which of these two possibilities was correct, we performed Northern blot analysis on glutamine synthetase (*femC*; also known as *glnA*) (Fig. 4). The data suggest that the first possibility is the more correct one; specifically, bacteria are responding to metabolomic changes by increasing transcription of genes necessary to counterbalance those changes. Interestingly, in untreated wild-type cultures, the post-exponential growth phase concentration of Glu and Gln increased between two and five times that of the exponential growth phase concentration (data not shown), and this increase correlated with a post-exponential growth phase decrease in *glnA* mRNA levels (Fig. 4). Similarly, Gln and Glu were not detected in the NMR spectra of the aconitase mutant strain, and this correlated with a high level of *glnA* mRNA in both the exponential and the post-exponential growth phases.

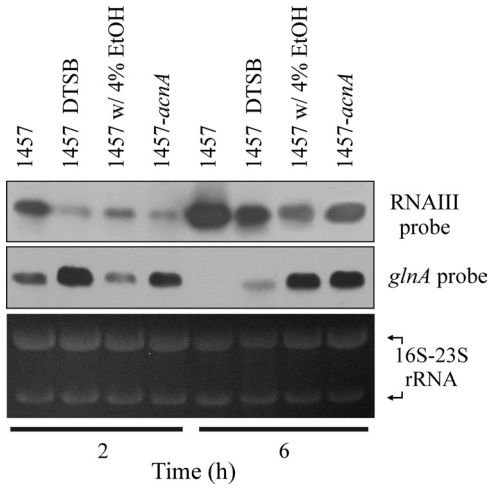

FIGURE 4. **Northern blot analysis of RNAIII and *glnA* mRNA levels in the exponential (2 h) and post-exponential (6 h) phases of growth.** To ensure that equivalent quantities of RNA were loaded in the gel, 23 S and 16 S rRNA were visualized by ethidium bromide staining and used as loading controls (*bottom panel*). The results are representative of at least two independent experiments.

The correlation between Gln and Glu concentrations and *glnA* mRNA levels is consistent with a GlnR-dependent regulation of *glnA* transcription (2). This correlation was maintained for Gln/Glu-sufficient or -insufficient conditions; however, the intermediate concentrations of Gln and Glu found during ethanol stress and iron-limited growth (data not shown) produce mixed *glnA* mRNA levels (Fig. 4). These data suggest that for the concentrations of Gln and Glu to affect *glnA* transcription, the stress-induced concentration change must be sufficiently large.

CcpA Responds to TCA Cycle-associated Metabolomic Changes—Ethanol stress, iron limitation, and TCA cycle inactivation increased the post-exponential growth phase concentration of glucose-6-phosphate (Table 2). Glycolytic intermediates such as glucose-6-phosphate and fructose-1,6-bisphosphate increase the ATP-dependent phosphorylation of the histidine-containing protein (HPr) by enhancing the activity of the HPr kinase (50). The increase in phosphorylated HPr enhances its interaction with the catabolite control protein A (CcpA) (51–53). CcpA primarily functions as a repressor; however, it also activates transcription of genes involved in fermentation and overflow metabolism (52, 54). In addition to the concentration of glucose-6-phosphate being increased by TCA cycle stress, the concentrations of several fermentation products or intermediates (*i.e.* lactate, acetate, and acetaldehyde) and the small phosphodonor acetyl phosphate (an indicator of overflow metabolism) were also increased (Table 1), consistent with a change in CcpA-mediated regulation. The repressor CodY also contributes to the regulation of overflow metabolism (54); however, CodY responds to the intracellular concentrations of branched chain amino acids (55). TCA cycle stress did not alter the concentrations of branched chain amino acids beyond the 5-fold threshold (Table 1), suggesting that the increase in overflow metabolism was independent of CodY.

In *Staphylococcus aureus*, CcpA enhances biofilm formation and PIA biosynthesis, whereas CodY represses PIA synthesis

(56, 57). In *S. epidermidis*, ethanol stress, iron limitation, and TCA cycle inactivation enhance biofilm formation and PIA synthesis (7, 13, 14, 16, 24, 58). Based on the metabolomic data and published observations, it was reasonable to hypothesize that PIA biosynthesis was regulated in response to TCA cycle-associated metabolomic changes by a CcpA-dependent and CodY-independent mechanism. To test this hypothesis, *ccpA* and *codY* deletion mutants were constructed in strains 1457 and 1457-*acnA*, and the amount of cell-associated PIA was determined after 6 h of growth (Fig. 5). Consistent with previous observations (7), TCA cycle inactivation (strain 1457-*acnA*) dramatically increased the accumulation of PIA, whereas neither CodY nor CcpA had a dramatic effect on the post-exponential growth phase amount of PIA. When the *codY* mutation was introduced into an aconitase mutant background, PIA accumulation resembled the response in strain 1457-*acnA*, suggesting that TCA cycle-associated changes in PIA biosynthesis are independent of CodY. In contrast to the *codY-acnA* double mutant, the *ccpA-acnA* double mutant failed to produce PIA, strongly suggesting that some TCA cycle-associated metabolomic changes (*i.e.* glucose-6-phosphate) are sensed by CcpA, which in turn activates PIA biosynthesis.

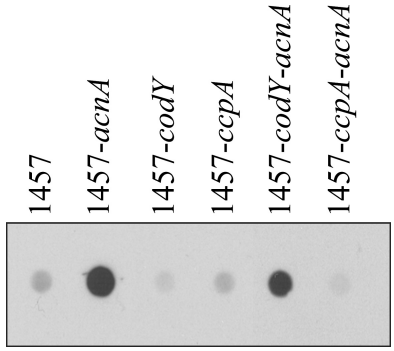

FIGURE 5. **CcpA is required for PIA synthesis during TCA cycle stress.** PIA immunoblot assay of strain 1457 and isogenic mutants of *acnA*, *codY*, *ccpA*, *codY*/*acnA*, and *ccpA*/*acnA* grown for 6 h in TSB. The results are representative of three independent experiments.

TCA Cycle Stress Decreases RNAIII Transcription—In *S. aureus*, inactivation of the TCA cycle increases the transcription or stability of the riboregulator RNAIII of the accessory gene regulator (Agr) system (8, 9). Conversely, increasing TCA cycle activity decreases the transcription or stability of RNAIII (59). The causal relationship between TCA cycle activity and RNAIII transcript levels in *S. aureus* led us to examine whether disparate environmental conditions would similarly affect RNAIII transcription or message stability in *S. epidermidis*. In contrast to *S. aureus*, TCA cycle inactivation decreased RNAIII transcription or stability during the exponential and post-exponential growth phases in *S. epidermidis* (Fig. 4). Importantly, ethanol stress and iron limitation decreased RNAIII transcription or stability in a similar manner to TCA cycle inactivation (Fig. 4). In total, these data suggest that environmental stresses act through the TCA cycle to elicit transcriptional changes to at least two of the major staphylococcal virulence regulators (*i.e.* CcpA and RNAIII).

DISCUSSION

In the life cycle of *S. epidermidis*, the transition from a skin-resident, commensal state to adhering on implanted biomaterials represents a dramatic environmental change. In most pathogenic bacteria, environmental changes are accompanied by changes in the transcription of virulence genes; thus, environmental signals (*e.g.* nutrient replete, iron-limiting, or oxygen-limiting growth conditions) commonly regulate virulence gene transcription (2, 60–64). Although *S. epidermidis* has relatively few virulence determinants, one of its primary pathogenic effectors is the exopolysaccharide PIA (65–68). Previously, we demonstrated that PIA biosynthesis is regulated by TCA cycle activity; specifically, repression of TCA cycle activity dramatically enhances transcription of PIA biosynthetic genes (*icaADBC*) and PIA accumulation (7, 24, 59). In this study, we demonstrate that dissimilar environmental signals decrease TCA cycle activity (Fig. 1), resulting in common metabolomic changes (Fig. 2 and Tables 1 and 2; summarized in Fig. 6) that alter the activity of metabolite-responsive regulators such as CcpA (Fig. 5). These data lead us to propose that it is the TCA cycle itself that is "sensing" the environmental transition and transducing this information into meta-

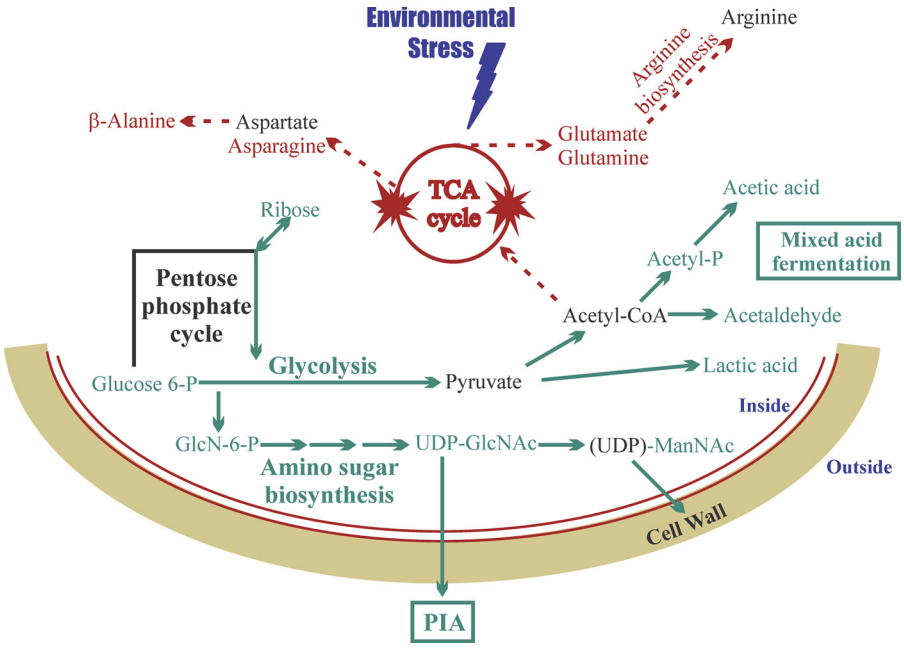

FIGURE 6. **Summary of post-exponential growth phase metabolic changes associated with TCA cycle stress.** Metabolites in *green* represent an increased concentration relative to the wild-type strain. Metabolites in *red* represent a decreased concentration relative to the wild-type strain. Metabolites and pathways in *black* are inferred from the data, but they are inconclusive. *Glucose-6-P*, glucose-6-phosphate; *GlcN-6-P*, GlcN-6-phosphate.

bolic signals that activate or repress the activity of metabolite-responsive regulators to modulate the expression of PIA and other virulence determinants.

As *S. epidermidis* transitions from residing on the skin to being implanted in a host, it enters into an environment where free iron is present at a concentration of 10^{-18} M (61), a condition antagonistic to TCA cycle activity (Fig. 1) (9, 11). Similarly, this transition dramatically decreases the availability of free oxygen (the partial pressure of atmospheric O_2 is 159 mm Hg at sea level, and this decreases to an estimated 3–5 mm Hg at the host cell level), a condition that is also antagonistic to TCA cycle activity. Taken together, this type of environmental transition is accompanied by conditions that are inhibitory to TCA cycle activity and stimulatory to PIA biosynthesis (7, 24). In other words, the transition from an external environment to an internal environment represses TCA cycle activity and primes *S. epidermidis* for PIA synthesis, which enhances biofilm formation and increases the likelihood of establishing a biomaterial-associated infection.

The significance of the data presented here is 5-fold. First, it establishes a mechanism by which well established regulators (*e.g.* CcpA) participate in responding to environmental stresses. Second, these data suggest how disparate environmental stimuli can cause common phenotypic changes (*e.g.* iron limitation and ethanol stress both increase PIA synthesis and biofilm formation (13, 69)). Third, these data suggest that a difficulty in attributing the effects of an environmental stimulus, such as iron limitation, to a specific regulator, such as the ferric uptake regulator (Fur) (70), is that many of the effects are due to metabolite-responsive regulators reacting to changes in the metabolome. Fourth, *S. epidermidis* has a second general stress response system that is largely independent of the σ^B-controlled general stress response (Fig. 2). Finally, in bacteria, three metabolic pathways (Embden-Meyerhof-Parnas, pentose phosphate, and TCA cycle) produce the 13 biosynthetic intermediates needed to synthesize all macromolecules in a bacterial cell. Therefore, by linking virulence factor synthesis to the TCA cycle, bacteria are connecting virulence to the availability of biosynthetic intermediates needed to synthesize virulence determinants.

CONCLUSION

TCA cycle stress alters the intracellular concentrations of metabolites (Tables 1 and 2) relative to those of the wild-type strain 1457. If the change in the concentration of a metabolite is sufficiently large, then the activity of a regulator that can respond to one of those metabolites may be altered. Therefore, these data present an exceptional opportunity to identify regulators that coordinate metabolism and virulence in *S. epidermidis*. Although a considerable amount of research needs to be done to determine which metabolite-responsive regulators are involved in responding to TCA cycle-associated metabolomic changes, the work presented here sheds light on how environmental signals alter the bacterial metabolic status to regulate adaptation to a new environment.

Acknowledgments—We thank the reviewers for their helpful suggestions for improving the manuscript.

REFERENCES

1. von Eiff, C., Peters, G., and Heilmann, C. (2002) *Lancet Infect. Dis.* **2,** 677–685
2. Somerville, G. A., and Proctor, R. A. (2009) *Microbiol. Mol. Biol. Rev.* **73,** 233–248
3. Begun, J., Sifri, C. D., Goldman, S., Calderwood, S. B., and Ausubel, F. M. (2005) *Infect. Immun.* **73,** 872–877
4. Coulter, S. N., Schwan, W. R., Ng, E. Y., Langhorne, M. H., Ritchie, H. D., Westbrock-Wadman, S., Hufnagle, W. O., Folger, K. R., Bayer, A. S., and Stover, C. K. (1998) *Mol. Microbiol.* **30,** 393–404
5. Mei, J. M., Nourbakhsh, F., Ford, C. W., and Holden, D. W. (1997) *Mol. Microbiol.* **26,** 399–407
6. Bae, T., Banger, A. K., Wallace, A., Glass, E. M., Aslund, F., Schneewind, O., and Missiakas, D. M. (2004) *Proc. Natl. Acad. Sci. U.S.A.* **101,** 12312–12317
7. Sadykov, M. R., Olson, M. E., Halouska, S., Zhu, Y., Fey, P. D., Powers, R., and Somerville, G. A. (2008) *J. Bacteriol.* **190,** 7621–7632
8. Somerville, G. A., Chaussee, M. S., Morgan, C. I., Fitzgerald, J. R., Dorward, D. W., Reitzer, L. J., and Musser, J. M. (2002) *Infect. Immun.* **70,** 6373–6382
9. Somerville, G. A., Cockayne, A., Dürr, M., Peschel, A., Otto, M., and Musser, J. M. (2003) *J. Bacteriol.* **185,** 6686–6694
10. Collins, F. M., and Lascelles, J. (1962) *J. Gen. Microbiol.* **29,** 531–535
11. Somerville, G., Mikoryak, C. A., and Reitzer, L. (1999) *J. Bacteriol.* **181,** 1072–1078
12. Varghese, S., Tang, Y., and Imlay, J. A. (2003) *J. Bacteriol.* **185,** 221–230
13. Knobloch, J. K., Bartscht, K., Sabottke, A., Rohde, H., Feucht, H. H., and Mack, D. (2001) *J. Bacteriol.* **183,** 2624–2633
14. Presterl, E., Suchomel, M., Eder, M., Reichmann, S., Lassnigg, A., Graninger, W., and Rotter, M. (2007) *J. Antimicrob. Chemother.* **60,** 417–420
15. Korem, M., Gov, Y., Shirron, N., Shuster, A., and Rosenberg, M. (2007) *FEMS Microbiol. Lett.* **269,** 153–159
16. Lyte, M., Freestone, P. P., Neal, C. P., Olson, B. A., Haigh, R. D., Bayston, R., and Williams, P. H. (2003) *Lancet* **361,** 130–135
17. Otzen, D. E., Sehgal, P., and Nesgaard, L. W. (2007) *Biochemistry* **46,** 4348–4359
18. Mack, D., Siemssen, N., and Laufs, R. (1992) *Infect. Immun.* **60,** 2048–2057
19. Handke, L. D., Slater, S. R., Conlon, K. M., O'Donnell, S. T., Olson, M. E., Bryant, K. A., Rupp, M. E., O'Gara, J. P., and Fey, P. D. (2007) *Can. J. Microbiol.* **53,** 82–91
20. Horton, R. M., Cai, Z. L., Ho, S. N., and Pease, L. R. (1990) *BioTechniques* **8,** 528–535
21. Kennedy, M. C., Emptage, M. H., Dreyer, J. L., and Beinert, H. (1983) *J. Biol. Chem.* **258,** 11098–11105
22. Baughn, A. D., and Malamy, M. H. (2002) *Proc. Natl. Acad. Sci. U.S.A.* **99,** 4662–4667
23. Lowry, O. H., Rosebrough, N. J., Farr, A. L., and Randall, R. J. (1951) *J. Biol. Chem.* **193,** 267–275
24. Vuong, C., Kidder, J. B., Jacobson, E. R., Otto, M., Proctor, R. A., and Somerville, G. A. (2005) *J. Bacteriol.* **187,** 2967–2973
25. Kay, L. E., Keifer, P., and Saarinen, T. (1992) *J. Am. Chem. Soc.* **114,** 10663–10665
26. Palmer, A. G., 3rd, Cavanagh, J., Wright, P. E., and Rance, M. (1991) *J. Magn. Reson.* **93,** 151–170
27. Bax, A., and Davis, D. G. (1985) *J. Magn. Reson.* **65,** 355–360
28. Forgue, P., Halouska, S., Werth, M., Xu, K., Harris, S., and Powers, R. (2006) *J. Proteome Res.* **5,** 1916–1923
29. Halouska, S., Chacon, O., Fenton, R. J., Zinniel, D. K., Barletta, R. G., and Powers, R. (2007) *J. Proteome Res.* **6,** 4608–4614
30. Halouska, S., and Powers, R. (2006) *J. Magn. Reson.* **178,** 88–95
31. Nguyen, B. D., Meng, X., Donovan, K. J., and Shaka, A. J. (2007) *J. Magn. Reson.* **184,** 263–274
32. Craig, A., Cloarec, O., Holmes, E., Nicholson, J. K., and Lindon, J. C. (2006) *Anal. Chem.* **78,** 2262–2267
33. Piotto, M., Saudek, V., and Sklenár, V. (1992) *J. Biomol. NMR* **2,** 661–665

34. Johnson, B. A. (2004) *Methods Mol. Biol.* **278,** 313–352
35. Cui, Q., Lewis, I. A., Hegeman, A. D., Anderson, M. E., Li, J., Schulte, C. F., Westler, W. M., Eghbalnia, H. R., Sussman, M. R., and Markley, J. L. (2008) *Nat. Biotechnol.* **26,** 162–164
36. Ulrich, E. L., Akutsu, H., Doreleijers, J. F., Harano, Y., Ioannidis, Y. E., Lin, J., Livny, M., Mading, S., Maziuk, D., Miller, Z., Nakatani, E., Schulte, C. F., Tolmie, D. E., Kent Wenger, R., Yao, H., and Markley, J. L. (2008) *Nucleic Acids Res.* **36,** D402–D408
37. Wishart, D. S., Tzur, D., Knox, C., Eisner, R., Guo, A. C., Young, N., Cheng, D., Jewell, K., Arndt, D., Sawhney, S., Fung, C., Nikolai, L., Lewis, M., Coutouly, M. A., Forsythe, I., Tang, P., Shrivastava, S., Jeroncic, K., Stothard, P., Amegbey, G., Block, D., Hau, D. D., Wagner, J., Miniaci, J., Clements, M., Gebremedhin, M., Guo, N., Zhang, Y., Duggan, G. E., Macinnis, G. D., Weljie, A. M., Dowlatabadi, R., Bamforth, F., Clive, D., Greiner, R., Li, L., Marrie, T., Sykes, B. D., Vogel, H. J., and Querengesser, L. (2007) *Nucleic Acids Res.* **35,** D521–D526
38. Kanehisa, M., Araki, M., Goto, S., Hattori, M., Hirakawa, M., Itoh, M., Katayama, T., Kawashima, S., Okuda, S., Tokimatsu, T., and Yamanishi, Y. (2008) *Nucleic Acids Res.* **36,** D480–D484
39. Karp, P. D., Ouzounis, C. A., Moore-Kochlacs, C., Goldovsky, L., Kaipa, P., Ahrén, D., Tsoka, S., Darzentas, N., Kunin, V., and López-Bigas, N. (2005) *Nucleic Acids Res.* **33,** 6083–6089
40. Werth, M. T., Halouska, S., Shortridge, M. D., Zhang, B., and Powers, R. (2010) *Anal. Biochem.* **399,** 58–63
41. Efron, B., Halloran, E., and Holmes, S. (1996) *Proc. Natl. Acad. Sci. U.S.A.* **93,** 13429–13434
42. Felsenstein, J. (1985) *Evolution* **39,** 783–791
43. Retief, J. D. (2000) *Methods Mol. Biol.* **132,** 243–258
44. Somerville, G. A., Saïd-Salim, B., Wickman, J. M., Raffel, S. J., Kreiswirth, B. N., and Musser, J. M. (2003) *Infect. Immun.* **71,** 4724–4732
45. Wu, S., de Lencastre, H., and Tomasz, A. (1996) *J. Bacteriol.* **178,** 6036–6042
46. Bischoff, M., Dunman, P., Kormanec, J., Macapagal, D., Murphy, E., Mounts, W., Berger-Bächi, B., and Projan, S. (2004) *J. Bacteriol.* **186,** 4085–4099
47. Bischoff, M., Entenza, J. M., and Giachino, P. (2001) *J. Bacteriol.* **183,** 5171–5179
48. Meier, S., Goerke, C., Wolz, C., Seidl, K., Homerova, D., Schulthess, B., Kormanec, J., Berger-Bächi, B., and Bischoff, M. (2007) *Infect. Immun.* **75,** 4562–4571
49. Pané-Farré, J., Jonas, B., Förstner, K., Engelmann, S., and Hecker, M. (2006) *Int. J. Med. Microbiol.* **296,** 237–258
50. Deutscher, J., and Saier, M. H., Jr. (1983) *Proc. Natl. Acad. Sci. U.S.A.* **80,** 6790–6794
51. Brückner, R., and Titgemeyer, F. (2002) *FEMS Microbiol. Lett.* **209,** 141–148
52. Sonenshein, A. L. (2007) *Nat. Rev. Microbiol.* **5,** 917–927
53. Warner, J. B., and Lolkema, J. S. (2003) *Microbiol. Mol. Biol. Rev.* **67,** 475–490
54. Shivers, R. P., Dineen, S. S., and Sonenshein, A. L. (2006) *Mol. Microbiol.* **62,** 811–822
55. Shivers, R. P., and Sonenshein, A. L. (2004) *Mol. Microbiol.* **53,** 599–611
56. Seidl, K., Goerke, C., Wolz, C., Mack, D., Berger-Bächi, B., and Bischoff, M. (2008) *Infect. Immun.* **76,** 2044–2050
57. Majerczyk, C. D., Sadykov, M. R., Luong, T. T., Lee, C., Somerville, G. A., and Sonenshein, A. L. (2008) *J. Bacteriol.* **190,** 2257–2265
58. Matinaho, S., von Bonsdorff, L., Rouhiainen, A., Lönnroth, M., and Parkkinen, J. (2001) *FEMS Microbiol. Lett.* **196,** 177–182
59. Zhu, Y., Xiong, Y. Q., Sadykov, M. R., Fey, P. D., Lei, M. G., Lee, C. Y., Bayer, A. S., and Somerville, G. A. (2009) *Infect. Immun.* **77,** 4256–4264
60. Bullen, J. J., Rogers, H. J., and Griffiths, E. (1978) *Curr. Top. Microbiol. Immunol.* **80,** 1–35
61. Litwin, C. M., and Calderwood, S. B. (1993) *Clin. Microbiol. Rev.* **6,** 137–149
62. Mekalanos, J. J. (1992) *J. Bacteriol.* **174,** 1–7
63. Park, M. K., Myers, R. A., and Marzella, L. (1992) *Clin. Infect. Dis.* **14,** 720–740
64. Milenbachs, A. A., Brown, D. P., Moors, M., and Youngman, P. (1997) *Mol. Microbiol.* **23,** 1075–1085
65. Vuong, C., Kocianova, S., Voyich, J. M., Yao, Y., Fischer, E. R., DeLeo, F. R., and Otto, M. (2004) *J. Biol. Chem.* **279,** 54881–54886
66. Vuong, C., Voyich, J. M., Fischer, E. R., Braughton, K. R., Whitney, A. R., DeLeo, F. R., and Otto, M. (2004) *Cell. Microbiol.* **6,** 269–275
67. Rupp, M. E., Ulphani, J. S., Fey, P. D., and Mack, D. (1999) *Infect. Immun.* **67,** 2656–2659
68. Rupp, M. E. (1997) in *The Staphylococci in Human Disease* (Crossley, K. B., and Archer, G. L., eds), pp 379–399, Churchill-Livingstone, New York
69. Deighton, M., and Borland, R. (1993) *Infect. Immun.* **61,** 4473–4479
70. Torres, V. J., Attia, A. S., Mason, W. J., Hood, M. I., Corbin, B. D., Beasley, F. C., Anderson, K. L., Stauff, D. L., McDonald, W. H., Zimmerman, L. J., Friedman, D. B., Heinrichs, D. E., Dunman, P. M., and Skaar, E. P. (2010) *Infect. Immun.* **78,** 1618–1628
71. Goddard, T. D., and Kneller, D. G. *Sparky 3*, University of California, San Francisco, CA

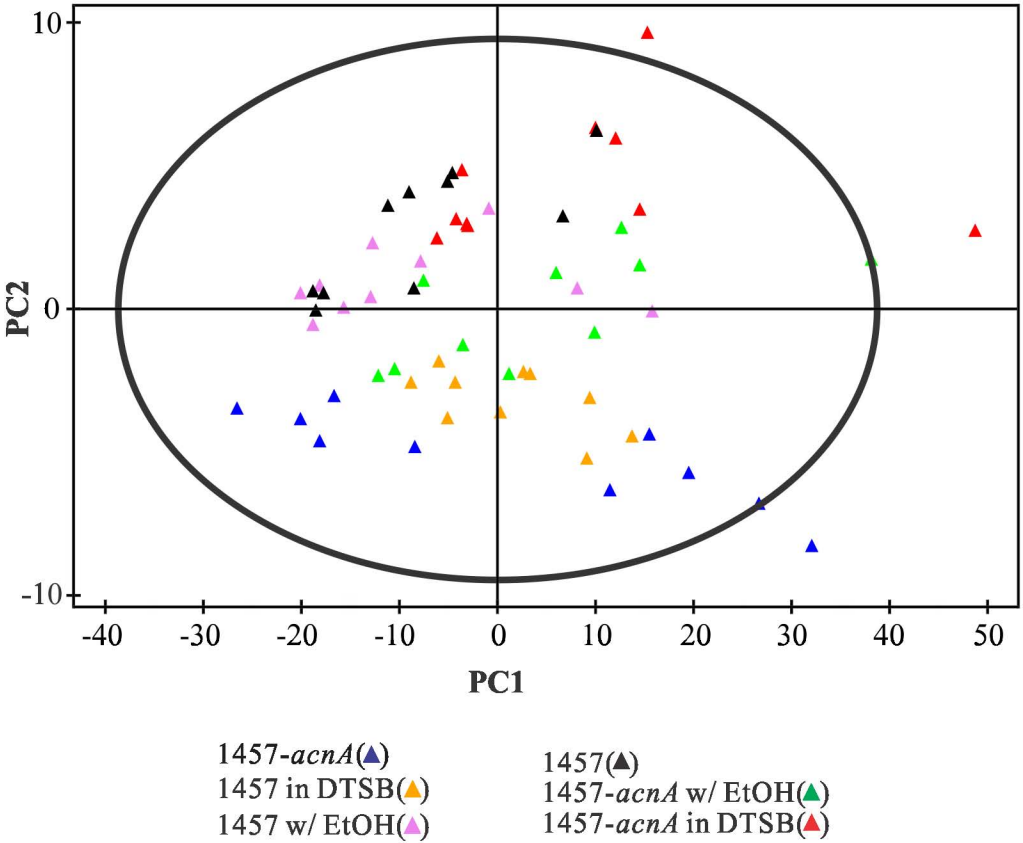

Figure S1. PCA 2D scores plot comparing non-stressed, ethanol stressed, or iron-limited cultures of strains 1457, 1457-*acnA*, and 1457-*sigB*::*dhfr* grown for 2 h. Symbols and colors are defined in the figure.